
Journal of Biological Physics **28:** 289–308, 2002.

Permeation Models and Structure-Function Relationships in Ion Channels

S. KUYUCAK and S.-H. CHUNG
Department of Theoretical Physics, Research School of Physical Sciences, Australian National University, Canberra, ACT 0200, Australia
E-mail: serdar.kuyucak0anu.edu.au; shin-ho.chung@anu.edu.au

Abstract. Recent determination of the molecular structures of potassium and mechanosensitive channels from x-ray crystallography has led to a renewed interest in ion channels. The challenge for permeation models is to understand the functional properties of channels from the available structural information. Here we give a critical review of the three main contenders, namely, continuum theories, Brownian dynamics and molecular dynamics. Continuum theories are shown to be invalid in a narrow channel environment because they ignore the self-energy of ions arising from the induced charges on the dielectric boundary. Brownian and molecular dynamics are thus the only physically valid methods for studying the structure-function relations in ion channels. Applications of these methods to potassium and calcium channels are presented, which illustrate the multi-ion nature of the permeation mechanism in selective biological channels.

Key words: Brownian dynamics, ion channels, molecular dynamics, permeation models, Poisson-Nernst-Planck equations

Abbreviations: PB – Poisson-Boltzmann; PNP – Poisson-Nernst-Planck; BD Brownian dynamics; MD – molecular dynamics

1. Introduction

A theoretical case for the existence of water filled holes in biological membranes was first made by Parsegian [1]. He observed that otherwise ions would have to overcome a self-energy barrier of 65 kT to cross the membrane, making this an extremely improbable event contrary to the observations that ions flow almost freely in and out of cells [2]. This was followed by many electrostatic calculations of potential energy profiles of single ions across schematic channels [3–7], mostly modeled after Gramicidin A because of its known structure [8]. The influence of the ionic atmosphere on the potential profiles was explored next using the Poisson-Boltzmann (PB) equation [9–11]. These results revealed substantial reductions in the single-ion potential energy profiles due to the shielding provided by the counter ions. Since then the PB equation has replaced Poisson's equation in potential energy calculations in numerous studies of ion channels [12–16]. In a parallel development, continuum theories of permeation such as Nernst-Planck

and Poisson-Nernst-Planck (PNP) equations were applied to ion channels to calculate their conductance properties (see [17, 18] for reviews and [19–24] for recent references). Unlike the popular rate theory, where the energy profile in a channel is determined by fitting it to the current-voltage ($I - V$) curve, the PNP theory actually calculates the potential for a given channel structure by solving Poisson's equation. In this sense, the PNP modeling of ion channels have been the first attempts at relating channel function to its structure.

The alternative to continuum theories are Brownian dynamics (BD) and molecular dynamics (MD) methods, where trajectories of individual ions are followed by computer simulations. Only ions' motion is followed in BD whereas all the atoms in a system are simulated in MD. Because these approaches are computationally very demanding, their application to realistic modeling of ion channels are much more recent. For example, while BD was proposed by Cooper *et al.* in 1985 using a structureless 1-dimensional channel [25], its application to realistic 3-dimensional channels appeared only in 1998 [26, 27]. Similarly MD have been used in simplified model studies of the gramicidin A channel from the eighties on (see [6, 28] for reviews). But the free-energy profiles obtained from these studies were mostly inconsistent with the experimental observations – the predicted barriers were too large to allow permeation of ions at the measured rates. The problem appears to be due to the simplifications made in the channel model and the force fields employed in MD simulations, forced by the limitations in computer power. With the current parallel and super computers, such simplifications are no more necessary, and the MD method could, in principle, yield more accurate results.

Determination of the crystal structures of the KcsA potassium [29] and mechanosensitive MscL channels [30] have shifted the focus of model studies from gramicidin A to these biological channels. The challenge for the permeation models is to relate the channel function to its underlying molecular structure. Properties such as $I - V$ curves and saturation of conductance with concentration are of primary importance in this regard. MD simulations are currently restricted to the nanosecond time regime. Therefore they cannot be used to calculate the channel conductance, and one has to resort to the coarser BD and PNP methods for this purpose. Solving the PNP equations is computationally much cheaper than the BD simulations, so, provided one could establish its validity in channels, it would be the method of choice. Here we present a critical review of the PNP, BD and MD methods and discuss their ability to model accurately the permeation process in ion channels. The BD method is shown to provide the best choice as demonstrated by applications to the potassium and calcium channels.

2. Permeation Models

We briefly introduce the basic formalism for the three permeation models PNP, BD and MD. The first two methods rely on continuum electrostatics to calculate the electric potential and field acting on ions. Here water, channel protein and mem-

brane are treated as continuous media with uniform dielectric constants, typically $\varepsilon_w = 80$ for water and $\varepsilon_p = 2$ for protein and lipid. Once the positions of fixed external charges in the protein and mobile ions in water are specified with charge densities ρ_{ex} and ρ_{el}, respectively, the potential φ is determined from the solution of Poisson's equation

$$\varepsilon_0 \nabla \cdot [\varepsilon(\mathbf{r}) \nabla \varphi(\mathbf{r})] = -(\rho_{ex} + \rho_{el}), \tag{1}$$

with appropriate boundary conditions. For an arbitrary channel boundary, Equation (1) can be solved numerically using the boundary element [3] or the finite difference [31] methods. Potential profiles obtained from such solutions indicate presence of significant self-energy (or reaction field) barriers due to the induced charges on the dielectric boundary that will prevent permeation of ions across a narrow pore. These barriers need to be canceled by attractive interactions with counter charges in the protein to make the channel operational.

In electrolyte solutions, mobile ions move to minimize the energy of the system and, at equilibrium, distribute themselves according to the Boltzmann factor

$$\rho_{el}(\mathbf{r}) = \sum_{\nu} z_\nu e n_{0\nu} \exp[-z_\nu e \varphi(\mathbf{r})/kT], \tag{2}$$

where $n_{0\nu}$ is the bulk (or reference) number density of ions of species ν and $z_\nu e$ is their charge. Substituting ρ_{el} in Equation (2) in Poisson's equation (1), one obtains the Poisson-Boltzmann equation for a $z : z$ electrolyte

$$\varepsilon_0 \nabla \cdot [\varepsilon(\mathbf{r}) \nabla \varphi(\mathbf{r})] = 2ezn_0 \sinh[ze\varphi(\mathbf{r})/kT] - \rho_{ex}. \tag{3}$$

The PB theory has been applied successfully to macromolecules, and this was deemed sufficient proof for its general validity including channels. However, there is a big difference between the two systems electrolytes are external to macromolecules and therefore self-energy of ions are negligible compared to their kinetic energy, whereas ions are surrounded by proteins in channels. This amplifies their self-energy by more than an order of magnitude to several kT, which is certainly not negligible. As shown by comparisons of PB and BD results [32], the potential barrier of a test ion is grossly underestimated in PB calculations because the self-energy is ignored in the continuum representation of ionic densities. As a result, counter ions freely enter the channel and shield the test ion, reducing the energy barrier it faces drastically compared to that of a single ion (zero concentration). This result cautions against the use of PB equation in narrow pores and also points to potential problems in application of PNP to channels.

2.1. PNP EQUATIONS

In continuum theories, the flux $\mathbf{J}_\nu$ of each ion species is described by the Nernst-Planck equation which combines the diffusion due to a concentration gradient with that from a potential gradient

$$\mathbf{J}_\nu = -D_\nu \left(\nabla n_\nu + \frac{z_\nu e n_\nu}{kT} \nabla \varphi \right), \tag{4}$$

where n_ν is the number density and D_ν is the diffusion coefficient of the ions of species ν, and we have used the Einstein relation $\sigma = (zen/kT)D$ to express the conductivity in terms of the diffusion coefficient. For self-consistency, Equation (4) needs to be solved simultaneously with Equation (1), and together they form the PNP equations. Because of their non-linear nature, the PNP equations can only be solved numerically using finite difference methods [22, 33]. In this regard, we note that the classic Goldman-Hodgkin-Katz equation [2] is, in fact, not a self-consistent solution of PNP because it assumes a constant electric field in disagreement with the solutions of Poisson's equation. Lack of analytical solutions has made it difficult to obtain an intuitive picture of ion permeation in the PNP approach.

Applications of PNP to ion channels have mostly focused on fitting the $I - V$ curves using the diffusion coefficients of ions as adjustable parameters. Since the $I - V$ curves are usually linear in the physiological range, such fits are trivial and tell us little about the capabilities of a model. In this respect, saturation of conductance with increasing concentration is a far more significant property that cannot be fitted by such a simple adjustment of parameters. Saturation arises because ions move in a single file and they have to overcome energy barriers in a channel. Thus there is a minimal time for each ion to cross the channel that puts an intrinsic limit on the amount of current it can carry regardless of how large the bath concentrations are. Because the channel current depends on the barrier height exponentially, the shape of the saturation curve is very sensitive to the details of the potential. Hence saturation rather than $I - V$ curves, provide the most stringent test on the validity of a permeation model. Surprisingly, saturation has been completely neglected in applications of PNP. Clues for reasons of this disregard may be found in the PNP equations and the potential profiles calculated from them. Inspection of Equation (4) gives no hints for the saturation behaviour. If anything, it suggests that conductance will rise linearly with concentration. Also the potential profiles calculated from PNP invariably exhibit deep wells without any barriers that are requisite for the onset of saturation. These strongly suggests that PNP will have problems in accounting for the saturation property of channels. After introducing BD, we will demonstrate through comparisons of PNP and BD that this is indeed the case.

2.2. BROWNIAN DYNAMICS

Brownian dynamics provides the most economical modeling for the permeation process in channels where ions are still described as individual particles rather than in continuum. Because the problem involves interaction of many ions with a complicated boundary and stochastic forces, no analytical solutions are possible, and one has to resort to computer simulations to calculate the channel observables. In BD simulations, the trajectory of each ion in a system of N ions is followed using the Langevin equation

$$m_i \frac{d\mathbf{v}_i}{dt} = -m_i \gamma_i \mathbf{v}_i + \mathbf{R}_i + \mathbf{F}_i, \quad i = 1, \ldots, N, \tag{5}$$

where m_i, $\mathbf{v}_i$ and γ_i are the mass, velocity and the friction coefficient of the ith ion. The three force terms on the r.h.s. of Equation (5) correspond to the frictional, random and the total systematic forces acting on the ion. The frictional and random forces represent the incessant collisions of the ion with the surrounding water molecules in an average way. Because they arise from the same source, the two forces are not independent but related through the fluctuation-dissipation theorem

$$m_i \gamma_i = \frac{1}{2kT} \int_{-\infty}^{\infty} \langle R_{ik}(0) R_{ik}(t) \rangle dt, \quad k = x, y, z. \tag{6}$$

Here the quantity in the integrand is the autocorrelation function of the random force and the angular brackets denote average over an equilibrium ensemble.

Calculation of the systematic forces both accurately and fast enough is a crucial requirement for the success of BD simulations. Ions are ultimately driven by the electric forces acting on them so they need to be calculated at an accuracy of a few percent. Solving Poisson's equation at such a precision at every time step would severely limit the total simulation time in BD, making it impossible to determine the conductance of a channel. This problem is circumvented by precalculating the electric potential and field on a grid of points and storing these values in a set of tables [34]. During simulations, the potential and field at desired points are determined by interpolating between the table entries. For calculational convenience, the total potential φ_i experienced by an ion i is broken into four pieces using the superposition principle

$$\varphi_i = \varphi_{X,i} + \varphi_{S,i} + \sum_{j \neq i} (\varphi_{C,ij} + \varphi_{R,ij}), \tag{7}$$

where the sum over j runs over all the ions in the system, and the four terms refer to:

i) $\varphi_{X,i}$ is the external potential due to the applied field, fixed charges in the protein, and the surface charges induced by these on the channel boundary. Because it is independent of ions, φ_X does not change during simulations. Poisson's equation

is solved in the absence of ions and the results at the grid points are stored in a 3-D table.

ii) $\varphi_{S,i}$ is the self-potential due to the charges induced by the ion i itself on the boundary. Poisson's equation is solved for a single ion with the applied field and fixed charges switched off. The ion is moved through the grid points and the calculated self-potentials are stored in a 3-D table (2-D if the channel boundary is axially symmetric).

iii) $\varphi_{C,ij}$ is the Coulomb potential due to the ion j. It is calculated directly from the Coulomb law.

iv) $\varphi_{R,ij}$ is the reaction potential due to the charges induced by the ion j. This is similar to the case *ii)* except a second ion is moved through all the grid points while the first one is hold at one point. Because the solution of Poisson's equation contains the Coulomb and self-potentials at the position i, these need to be subtracted to obtain $\varphi_{R,ij}$. The results are stored in a 6-D table (5-D if the boundary is axially symmetric).

An identical procedure is used to store the three components of the electric field on three sets of tables. Tests indicate that forces acting on ions in channels can be calculated very accurately with this method [34]. In addition to the electric forces, ions also experience short-range forces when they are close to other ions or protein walls. These are typically modeled by two-body potentials with an r^{-9} dependence. More sophisticated forms determined from the MD simulations are also employed and are, in fact, found to be necessary in modeling of multi-ion channels [35].

To complete the simulation system, electrolyte filled reservoirs are attached on either side of the lipid-channel complex. From Debye screening arguments, the optimal size for the reservoirs is about 30 Å for physiological concentrations (0.15 M). Concentrations of ions in the reservoirs are maintained at the specified values by elastically scattering them off the boundaries. When an ion crosses the channel, an ion of the same species is transplanted to the other side so as to keep the concentrations at their specified values. This process simply mimics the completion of the circuit by a wire in an actual conduction experiment. Finally, the membrane potential is implemented by applying a uniform electric field across the simulation system. Once the system is equilibrated in BD simulations, charge separation occurs across each reservoir so as to cancel the applied field. Thus the potential drop occurs mainly across the channel. We calculate this potential drop from the difference of the average potential values at the centers of the reservoirs, similar to measuring the voltage difference between the two sides of a membrane with the probes of a voltmeter.

What are the limitations of BD? The precise answer depends on how one calculates the systematic forces. The only phenomenological parameter in the Langevin equation (5) is the diffusion coefficient of ions, which can be easily estimated from MD simulations. If one could also calculate the average forces acting on ions from MD simulations, BD would become a very rigorous method and give similar results as MD. At present, this level of rigor has not been achieved yet,

and continuum electrostatics is employed in force calculations. Applicability of continuum electrostatics in channels is by no means a settled issue as one can present arguments either way. Further study of this problem using MD simulations is required to reach a definite conclusion. In the mean time, applications of BD to channels that use continuum electrostatics are quite successful and, with the exception of the gramicidin A channel, do not provide any evidence that may point to its failure.

2.3. COMPARISON OF PNP AND BD

In the PNP approach, ion concentration and flux are described by continuous quantities corresponding to macroscopic, space-time averages of microscopic motion of individual ions. This averaging, called mean field approximation, is known to be valid in bulk electrolytes where many ions participate and their interaction with the system boundaries are negligible. The situation in channels is quite the opposite – there are only a few ions and they interact strongly with the channel boundary. Could one still expect PNP to work under these conditions? Until recently, this question has been ignored by the practitioners of PNP, who offered the successful fitting of the experimental $I - V$ curves for justification of the theory. Here we demonstrate that one of the primary contributions to the potential energy – the self energy arising from the charges induced by the ion on the dielectric boundary – is completely neglected in PNP. Therefore it cannot give a valid description of ion permeation in narrow pores.

The simplest way to test this assertion is to compare the PNP and BD predictions in two cases: i) the dielectric constant of protein is set to $\varepsilon_p = 80$ so that there is no self-energy barrier for permeating ions, ii) the usual case with $\varepsilon_p = 2$ when the ions experience the full impact of the self-energy barrier. For simplicity, the comparisons are carried out using a 35 Å long cylindrical channel with a variable radius. As shown in Figure 1, the two theories agree in case (1) regardless of the pore radius, but a large discrepancy occurs in case (ii) at small radii. The suppression of current in BD in the latter case is simply due to the large self-energy barriers ions face in narrow pores. The fact that PNP gives more or less the same conductance in both cases proves that the self-energy of ions is ignored in PNP. With increasing pore radius, the self-energy contribution rapidly decreases, and the PNP and BD results are seen to merge for $r > 10$ Å. The biological ion channels have much smaller radii, therefore they are outside the domain of validity of PNP.

Earlier we have stressed the importance of describing the saturation of conductance with increasing concentration in model studies, and conjectured that PNP is likely to fail in this respect because the self-energy barriers are ultimately responsible in limiting the transition rate of ions in a channel. We illustrate this point here using a cylindrical channel as above with $r = 4$ Å. In order to make it conduct cations, negative charges of magnitude $-0.72\ e$ are distributed at the mouths of the channel, which is sufficient to cancel the self-energy barrier. In Figure 2, we

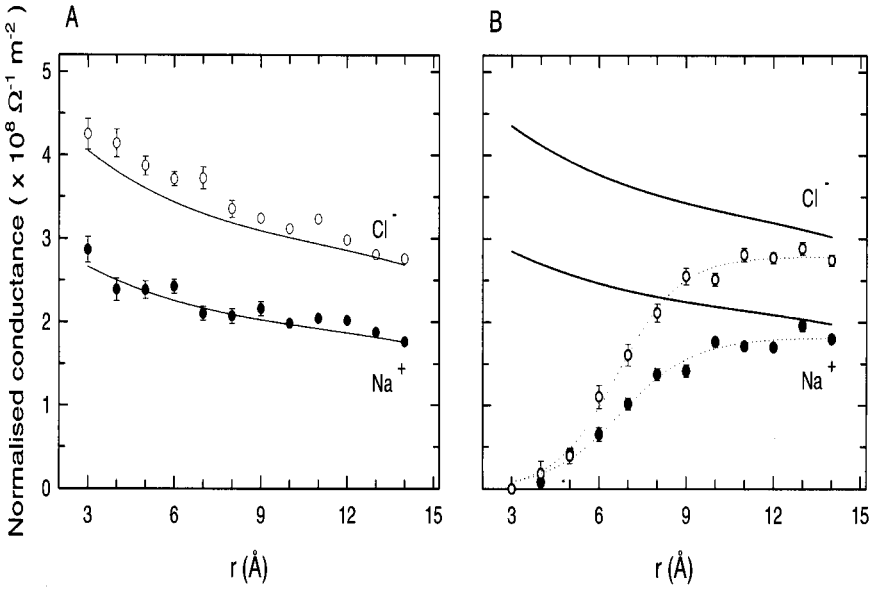

Figure 1. Comparison of conductance of Na^+ and Cl^- ions predicted by PNP (solid lines) and BD (circles fitted by dotted lines) in cylindrical channels with a varying radius. The conductance values are normalised by dividing with the cross-sectional area. A symmetric NACl solution of 0.3 M and an applied potential of 0.1 V are used. On the left, ε_p for the channel protein is set to 80 so that there is no self-energy barrier for ions. The realistic case with $\varepsilon_p = 2$ is shown on the right.

compare the PNP and BD results for conductance-concentration curves. The BD results are just as one would expect from a cation selective channel: chloride ions do not conduct and the sodium conductance saturates at about 150 pS. In stark contrast, PNP predicts a linearly rising conductance for both sodium and chloride ions beyond a transient regime at low concentrations. The initial asymmetric behaviour happens because the channel is negatively charged and exhibits some degree of selectivity until it attains electroneutrality. Although we have used a schematic channel to demonstrate our point, inability of PNP to describe saturation is a generic future that applies to any channel model; the highly-charged, multi-ion KcsA potassium channel being an extreme example [33].

There are important lessons to be learned from the brief history of PNP in channels with regard to the modeling of biological systems. One should definitely strive to explain the available experimental data, but not just a selected set that appears to give good results. When a model fails to account for a particular feature, it could simply be due to inadequate parameterization or oversimplification that may ultimately be resolved by a more careful study. But if the problem persists after such refinements, it is likely to be signaling a more fundamental short-coming of

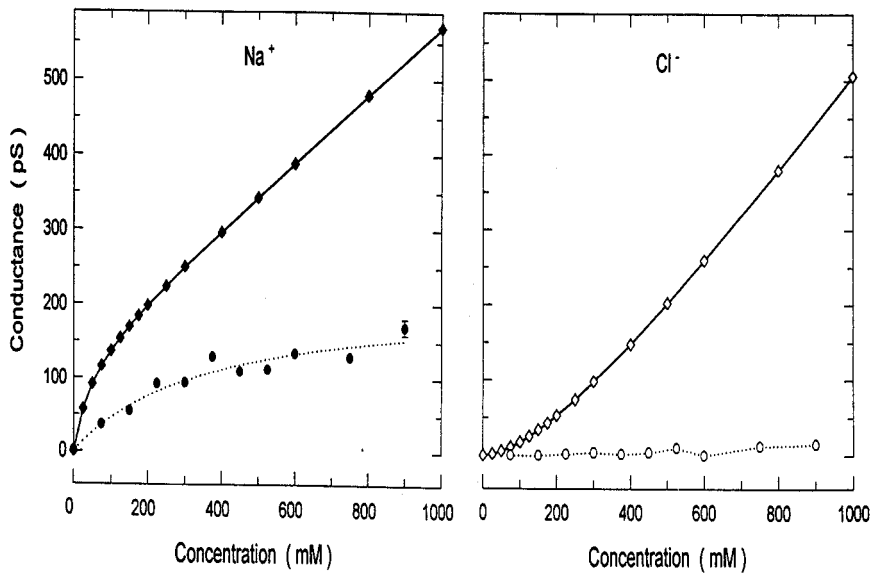

Figure 2. Conductance-concentration curves for Na^+ and Cl^- ions in PNP (diamonds fitted with solid lines) and BD (circles fitted with dotted lines) in a $r = 4$ Å channel with fixed charges. Symmetric solutions and an applied potential of 0.1 V are used.

the model that needs to be explored further by appealing to a higher level of theory. Had this been done in applications of PNP to channels, so much effort would not have been wasted in pursuing it.

2.4. MOLECULAR DYNAMICS

Compared to PNP and BD, the MD method is both more fundamental and conceptually simpler: one solves Newton's equation of motion for all the atoms in the system

$$m_i \ddot{\mathbf{r}}_i = -\nabla_i U(\{\mathbf{r}_i\}), \tag{8}$$

and traces their motion via computer simulations. Here m_i refer to the mass of atoms, $\mathbf{r}_i$ to their coordinates and $U(\{\mathbf{r}_i\})$ is the potential function for the system whose gradient specifies the force acting on individual atoms. Typically, U is taken as pair-wise sum of the Coulomb and Lennard-Jones potentials. There are two limitations of MD that prevents it from becoming the model of choice in permeation studies. The first is practical: MD simulations can be run for nanoseconds using present computers whereas many microseconds is required to determine the conductance of a channel. Even if the computer speeds keep increasing at current rates, it will take decades to reach that level of performance. The second is to do

with the force fields employed in the MD simulation packages that do not include the polarization effects explicitly. Polarization interaction constitutes a significant part of the total energy of a water molecule or ion, but because it is expensive to calculate nonadditive forces, it is treated approximately by absorbing its effects in the Coulomb and Lennard-Jones potentials. This may be fine in a bulk-like environment but during permeation, ions move from bulk water into a channel which has very different polarization characteristics. Therefore it is very important to develop polarizable force fields in order to obtain realistic free-energy profiles of ions in channels. The computational resources required for this purpose is now within the reach of current parallel and super computers, and we can expect this aim to be achieved in near future.

Because of the time limitation, the use of MD in channels is restricted to calculation of free energy profiles of ions and some other quantities related to permeation (e.g. ordering of water molecules, diffusion coefficients). In this respect, it plays a complimentary role to the BD simulations by providing the required input parameters such as the diffusion coefficients of ions and the effective dielectic constant of water in the channel. Also, size based selectivity of ions cannot be described in BD, so the free-energy perturbation calculations from MD simulations are required to explain this property.

3. Applications to Specific Channels

Because of its known structure, a great deal of effort went into model studies of the gramicidin A channel in the past. The expectation was that one would gather useful insights about the permeation process in biological channels from such studies. With the appearance of the structure of the KcsA potassium channel, we now know that gramicidin A is rather remote and isolated case, and is not likely to shed much light to other channels. Here we consider KcsA potassium and L-type calcium channels to illustrate how channels reconcile the two conflicting requirements – fast permeation demanding a relatively flat potential vs. selectivity requiring a deep binding site – by using a multi-ion permeation mechanism.

3.1. KCSA POTASSIUM

The determination of the crystal structure of the KcsA potassium channel [29] has given a new impetus to modeling of ion channels. While KcsA is a bacterial potassium channel, quite different from those found in animals in many details (e.g. gating), two of its main features are expected to be preserved in all potassium channels, namely, the narrow selectivity filter with a 1.5 Å radius that holds two K^+ ions, and a water filled cavity that follows it (see the inset in Figure 3). The role of the filter is to select the K^+ ions against Na^+ and the cavity helps in reducing the self-energy barrier of ions [36]. Here we present the results of BD and MD studies of the KcsA channel.

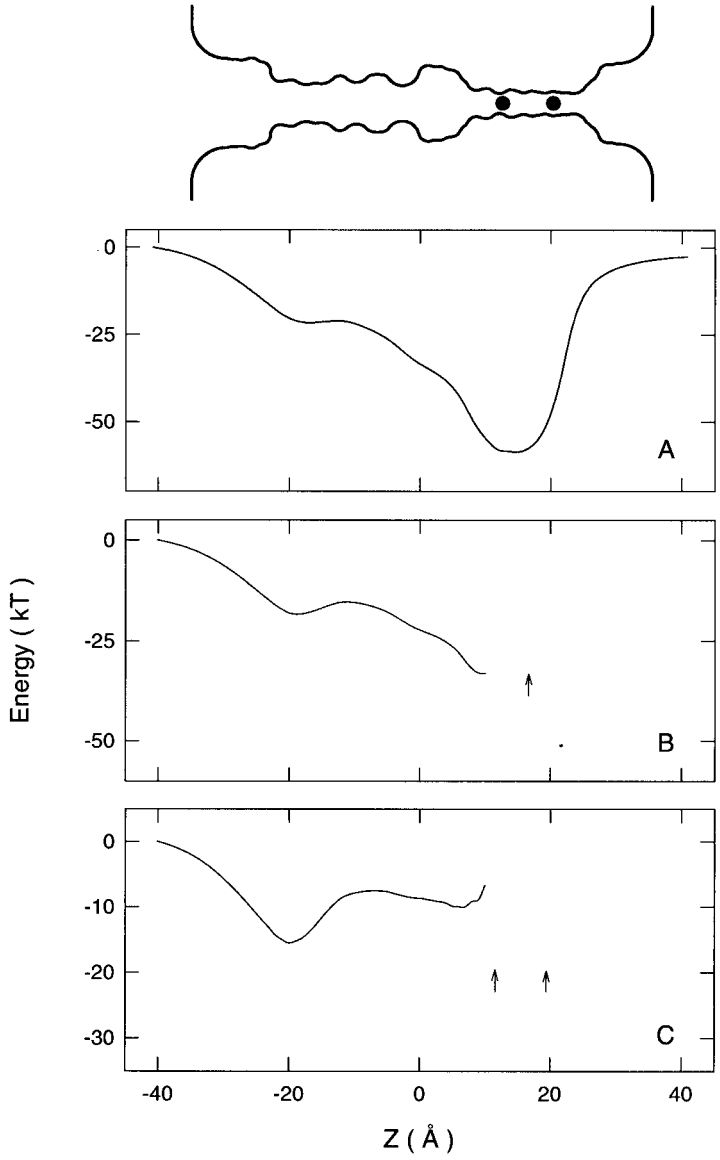

Figure 3. Potential energy profiles of a K^+ ion traversing the KcsA channel under an applied field of 10^7 V m^{-1} when there are 0 (A), 1 (B) and 2 (C) resident ions in the channel. The dielectric constants used in the solution of Poisson's equation are 60 for channel water and 2 for the protein. The electric field is in the z direction driving ions from inside the cell (left) to outside (right). The upward arrows indicate the location of the resident ions when the test ion is at the center of the channel ($z = 0$ Å). The schematic channel in the inset shows the positions of the ions in case C.

The first BD study of KcsA was carried out using a simplified pore shape and representing the charge residues on carbonyl groups in the selectivity filter and in the inner and outer mouths with dipoles [37]. This was followed by a more sophisticated study that included all the experimentally-determined channel protein in the model structure [38]. As the crystal structure of KcsA corresponds to its closed state, open-state configurations were constructed via MD simulations. The refinement has led to a better description of some properties (e.g. positions of the K^+ ions in the channel were in better agreement with the experimentally observed sites) but otherwise corroborated the permeation mechanism found in the earlier study. We give an intuitive illustration of this mechanism using the multi-ion potential profiles obtained by minimizing the energies of ions resident in the channel while another ion is brought in the channel in small steps (Figure 3). As seen in diagram A, there is a very deep well (67 kT) for a single K^+ ion that will permanently bind it to the selectivity filter. The potential profile of a second ion (B) in the presence of the first one is again attractive though the well depth is reduced by about half. A third K^+ ion is still attracted to the channel from the intracellular side but now it faces a barrier of several kT high. Once it goes over this barrier through thermal fluctuations, it moves rapidly under the potential gradient towards the selectivity filter and destabilizes the equilibrium of the two resident ions there. From this point on, the three ions move more or less in tandem to the right until the right-most one is expelled from the channel, leaving again two K^+ ions in the filter.

This qualitative account of the permeation process in KcsA has been made quantitative by trajectory analysis of the BD simulations [37, 38]. For example, the average concentration of ions in the channel, the average time an ion spends in various parts of the pore, and its mean velocity provide complementary information about the ion dynamics. In the presence of a driving field, two ions are found in the filter and one near the inner mouth (cf. Figure 3C). Ions spend the most time in accessing the channel and climbing over the central barrier, the remaining time being negligible in comparison. As the first process depends on the concentration and the second does not, this provides a natural explanation for the saturation of current with increasing concentration. Similarly, analysis of the mean velocities shows that ions move at a fraction of their drift velocity in bulk while climbing the barrier but once over, they move an order of magnitude faster. This explains the observed insensitivity of calculated current to diffusion coefficient of ions employed in BD simulations – a welcome result considering the uncertainties in the estimated values of diffusion coefficients from MD (see below).

The permeation mechanism delineated by the potential energy profiles and the BD simulations sheds much light into the central paradox in operation of ion channels (i.e. large conductance vs. selectivity), and how nature has solved this problem. The selectivity filter is very narrow to enable it to differentiate between potassium and sodium ions, and it has a very deep binding site. On the basis of these two factors, one would intuitively expect ions' crossing of the filter to be

the rate-limiting step in the permeation process. In fact, Coulomb repulsion in the three-ion system causes it to be unstable and thereby making this the fastest step in permeation. A related puzzle is the large variations (nearly two orders of magnitude) observed in the conductance levels of various potassium channels. Clearly one could not explain such a diversity, had the filter been the rate limiting step because it is presumed to be conserved. Study of multi-ion potential profiles show that the energy barrier in KcsA can be reduced substantially by increasing the radius of the inner mouth of the channel by a few Å, which leads to an exponential increase in conductance [38]. Thus the large conductance variations in potassium channels can be explained by changes in the radius of the intracellular mouth while keeping the selectivity filter on the opposite side intact.

The physiological properties of KcsA such as $I - V$ and $G - c$ curves have also been determined from the BD simulations [37, 38]. The calculated conductance G and half-saturation c_s, values are found to be within the observed range [39, 40].

Many MD studies of the KcsA channel have been performed since the appearance of its structure (see [41] for a review). Most of them focus on free-energy calculations of K^+ ions in the selectivity filter. There is a general agreement among the MD simulations that the KcsA protein can hold three K^+ ions in a stable conformation, two in the filter and one in the central cavity, as observed in the x-ray structure [29]. However, in view of the uncertainties associated with the nonpolarizable force fields employed in these studies, the absolute values of the calculated free energies has to be interpreted with caution.

A more rewarding quantity to study with MD is the selectivity of KcsA because it cannot be described in BD and also it involves differences in free energies, hence suffers less from the defects in force fields. Free energy perturbation calculations for the transformation $K^+ \rightarrow Na^+$ predict relative barriers of $\sim 8\ kT$ for sodium permeation, [43], sufficient to explain the observed selectivity margin of 10^4. Further study of coordination of potassium and sodium ions in the filter shows that the carbonyl oxygens provide a bulk-like solvation environment for K^+ but fail to do so for Na^+ [42, 43]. According to the picture emerging from these studies, the filter is quite rigid and its size is optimized for solvation of the K^+ ions (radius 1.33 Å). Therefore the smaller Na^+ ions with radius 0.95 Å are not as well hydrated and rejected from the channel.

Diffusion of ions and water in KcsA have also been studied with MD [42, 43]. The main finding from these studies is that diffusion coefficient of K^+ ions is suppressed down to about 10% of the bulk value in the filter region but remains relatively high ($>$ 50% of bulk value) in the rest of the channel. As mentioned in the discussion of BD results, permeation dynamics in the filter region is dominated by Coulomb repulsion during a conduction event, and despite the large suppression of the diffusion coefficient, this is actually the fastest step in permeation. Motion of individual ions in the channel has been discussed in some MD studies of KcsA. However, such single-event studies have little meaning statistically, and cannot not be used to draw conclusions about permeation dynamics.

3.2. L-TYPE CALCIUM

Calcium channels are as ubiquitous in excitable cells as potassium channels and share similar properties, that is, they are extremely selective (margin for Ca/Na is 10^3) and yet conduct at the picoampere level [44]. But there is also a crucial difference: selectivity is based on charge and not size. Radius of the Ca^{2+} ion (0.99 Å) is only slightly larger than that of Na^+ while the pore radius is estimated to be about 2.8 Å [45]. Thus selectivity of calcium channels can be understood at the BD level without having to appeal to MD. An intriguing feature of this selectivity against Na^+ ions is that it is contingent upon the presence of Ca^{2+} ions. In their absence, Na^+ ions conduct at an even faster rate than Ca^{2+}. Physiological properties of calcium channels are well known but the corresponding information on the structural side is rather scarce, i.e. their tertiary structures have not been determined from crystallography yet. This discourages any attempts to model calcium channels using MD simulations because they are quite sensitive to structural details, and it would be very difficult to get sensible results out of MD in such circumstances. Fortunately, structural requirements for BD simulations are much less demanding – an approximate shape of the channel and positions of the partial charges in the protein are all one needs to model its functional properties. Such an attempt has recently been made in a model study of L-type calcium channel [35].

The shape of the calcium channel used in the model study is shown in the inset of Figure 4. It is inspired by the KcsA structure but modified to take into account a variety of physiological data. Four glutamate residues are known to play an essential role in the channel conductivity and selectivity [46], and these are represented by four negative charges in the narrow selectivity filter (indicated by squares in the figure). The only other charge residues required to make the channel conduct are the set of four dipoles placed on the intracellular mouth (diamonds in the figure). As in the KcsA study, multi-ion potential profiles give an intuitive understanding of the permeation mechanism in the calcium channel. As shown in Figure 4A, a single Ca^{2+} ion would be deeply bound (58 kT) in the selectivity filter. A second Ca^{2+} ion is attracted to the channel from the extracellular (right) side, and the two ions can coexist in the filter region in a semi-stable equilibrium, until the resident ion on the left climbs over the barrier of 5 kT via thermal fluctuations and exits the channel. A similar picture is obtained for the Na^+ ions (B), except three of them can coexist in the filter and the final barrier to permeation is only 1 kT, which explains why the sodium ions conduct faster. Selectivity of the calcium channel can be understood by constructing multi-ion profiles with mixed set of ions (Figure 4C). When a Na^+ ion is resident in the filter, a Ca^{2+} ion is attracted to the filter and expels the Na^+ ion from the channel upon entry. A similar result is obtained when there are two Na^+ ions in the filter. In the reverse case of a Ca^{2+} ion in the filter, though a Na^+ ion is still attracted, it is unable to push the Ca^{2+} ion over the large barrier of 16 kT. Thus once a Ca^{2+} ion enters the channel, Na^+ ions cannot push it out, only another Ca^{2+} ion can achieve that feat. This gives a simple explanation of the selectivity

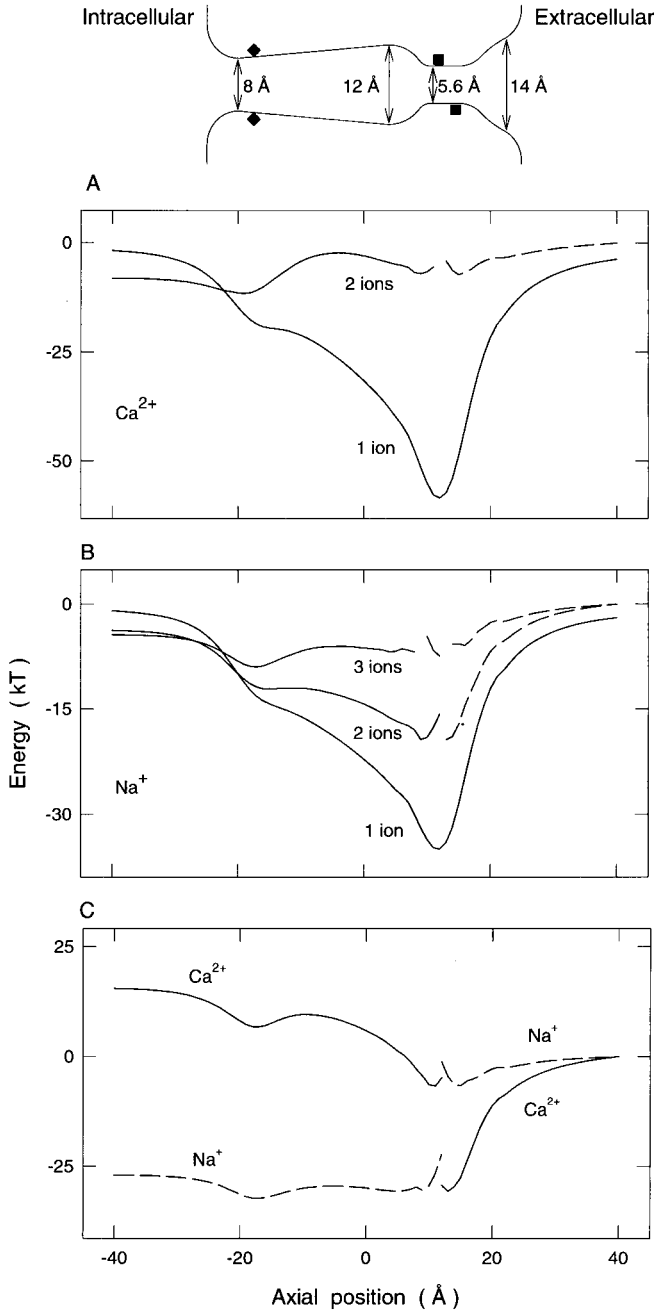

Figure 4. Shape of a model calcium channel and locations of charge residues (inset). Potential energy profiles for 1 and 2 Ca^{2+} ions (A), and 1, 2 and 3 Na^{+} ions (B). The profiles for the mixed system is shown in C. The parameters are as in Figure 3 except the electric field is reversed to the inward direction (right to left).

mechanism in calcium channels in terms of the electrostatic interactions of ions, which is in conformity with the insights gathered from the rate theory models.

A number of physiological properties of calcium channels have been determined from the BD simulations [35]. For example, the $I - V$ and $G - c$ curves are found to be in good agreement with the experimental observations. We will not dwell on these standard quantities here but rather discuss a few other exotic properties of calcium channels that have been elucidated by these calculations. The first is the anomalous mole fraction effect, so called because the channel current vanishes at a certain range of Ca^{2+} concentrations in the presence of a fixed 0.15 M Na^{+} as shown in the inset of Figure 5A. The BD results indicate that the rapid drop and subsequent vanishing of the channel current is due to the blocking of Na^{+} current by Ca^{2+} ions. Once the Ca^{2+} concentration is high enough to allow two Ca^{2+} ions in the filter, the channel starts conducting again but now Ca^{2+} ions instead of Na^{+}. While sodium ions cannot block calcium, their presence in the vestibule can nevertheless slow down entry of a second Ca^{2+} ion necessary for conduction. As illustrated in Figure 5B, the predicted reduction in the channel current with increasing Na^{+} concentration is in excellent agreement with the experimental data. A final example is the effect of mutating one of the glutamate residues to neutral glutamine on the blocking of Na^{+} current (Figure 5C). The mutation leads to a reduction in the depth of the potential well compared to the native case so that entry of a Ca^{2+} ion in the channel is delayed, and the blocking occurs at a higher Ca^{2+} concentration. Trends in the data (inset of C) is again reproduced by the BD simulations.

4. Conclusions

The main conclusion of this work is that Brownian dynamics currently provides the best alternative for studying structure-function relations in ion channels. Continuum theories are ruled out because they ignore self-energy which is responsible for many properties such as saturation of conductance through creation of energy barriers. Molecular dynamics, although more fundamental than BD, is unable to calculate the key property of channels (i.e. conductance), hence it is of limited use for the above purpose. Studies of potassium and calcium channels using continuum electrostatics and BD demonstrate that permeation mechanism involves multi-ions, and Coulomb repulsion among the ions plays an essential role in explaining the central paradox of ion channels, that is, the fast permeation of ions across a binding site (i.e. the selectivity filter). Comparisons of BD simulation results to experimental observations are very encouraging for future applications of this method as they indicate that basic properties of ion channels can be understood using a simplified model in the absence of a detailed tertiary structure.

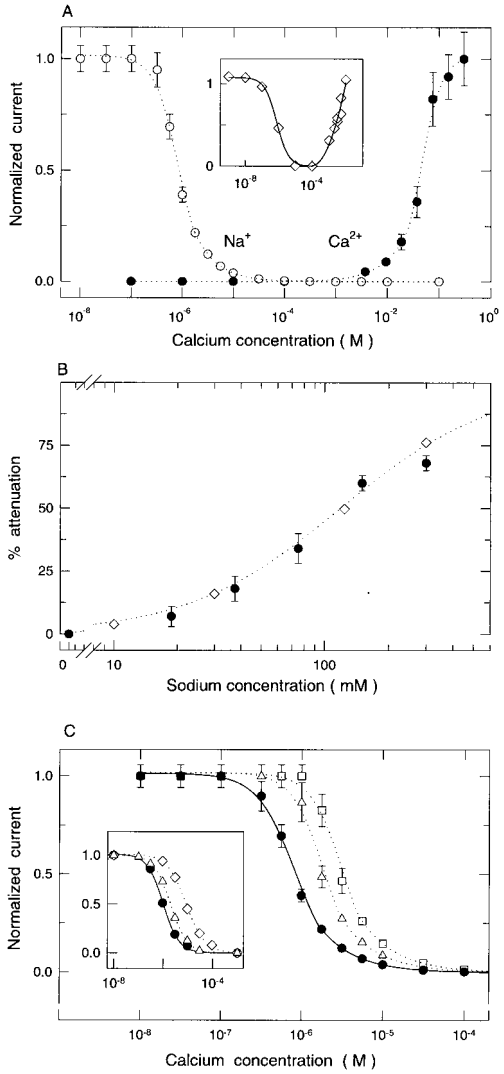

Figure 5. (A) Mole fraction effect. Ca^{2+} (filled circles) and Na^{+} (open circles) current passing through the channel normalized by the maximum value of each is plotted against the Ca^{2+} concentrations while keeping the Na^{+} concentration fixed at 0.15 M. Experimental results from [47] are shown in the inset. (B) Attenuation of Ca^{2+} current by Na^{+} ions. The percentage reduction in the channel current is plotted against Na^{+} concentration while the Ca^{2+} concentration is fixed at 0.15 M (filled circles). The open diamonds and dotted line show the experimental data from [48]. (C) The effect of removing glutamate charges on channel selectivity. The Na^{+} current passing through the channel at different Ca^{2+} concentrations with all four glutamate charges in place (filled circles), the outermost glutamate removed (triangles) and the innermost glutamate removed (squares), otherwise all conditions are as in A. Experimental data for wild type (filled circles) and for single glutamate to neutral glutamine mutations of two different residues (triangles and diamonds) are shown in the inset [46]. In all cases a driving potential of –0.2 V is applied.

References

1. Parsegian, A.: Energy of an ion crossing a low dielectiic membrane: solutions to four relevant electrostatic problems, *Nature* **221** (1969), 844–846.
2. Hille, B.: *Ionic Channels of Excitable Membranes*, 2nd ed., Sinauer Associates, Sunderland, MA, 1992.
3. Levitt, D.G.: Electrostatic calculations for an ion channel. I. energy and potential profiles and interactions between ions, *Biophys. J.* **22** (1978), 209–219.
4. Jordan, P.C.: Electrostatic modeling of ion pores. Energy barriers and electric field profiles, *Biophys. J.* **39** (1982), 157–164.
5. Monoi, H.: Effective pore radius of the gramicidin channel. Electrostatic energies of ions calculated by a three-dielectric model, *Biophys. J.* **59** (1991), 786–794.
6. Partenskii, M.B. and Jordan, P.C.: Theoretical perspectives on ion-channel electrostatics: continuum and microscopic approaches, *Q. Rev. Biophys.* **25** (1992), 477–510.
7. Hoyles, M., Kuyucak, S. and Chung, S.H.: Energy barrier presented to ions by the vestibule of the biological membrane channel, *Biophys. J.* **70** (1996), 1628–1642.
8. Urry, D.W.: The gramicidin A transmembrane channel: a proposed π_{LD} helix, *Proc. Natl. Acad. Sci. USA* **68** (1971), 672–676.
9. Levitt, D.G.: Strong electrolyte continuum theory solution for equilibrium profiles, diffusion limitation, and conductance in charged ion channels, *Biophys. J.* **48** (1985), 19–31.
10. Jordan, P.C., Bacquet, R.J., McCammon, J.A. and Tran, P.: How electrolyte shielding influences the electrical potential in transmembrane ion channels, *Biophys. J.* **55** (1989), 1041–1052.
11. Cai, M. and Jordan, P.C.: How does vestibule surface charge affect ion conduction and toxin binding in a sodium channel, *Biophys. J.* **57** (1990), 883–891.
12. Sankararamakrishnan, R., Adcock, C. and Sansom, M.S.P.: The pore domain of the nicotinic acetylcholine receptor: molecular modeling, pore dimensions, and electrostatics, *Biophys. J.* **71** (1996), 1659–1671.
13. Weetman, P., Goldman, S. and Gray, C.G.: Use of Poisson-Boltzmann equation to estimate the electrostatic free energy barrier for dielectric models of biological ion channels, *J. Phys. Chem.* **101** (1997), 6073–6078.
14. Adcock, C., Smith, G.R. and Sansom, M.S.P.: Electrostatics and the ion selectivity of ligand-gated channels, *Biophys. J.* **75** (1998), 1211–1222.
15. Cheng, W., Wang, C.X., Chen, W.Z., Xu, Y.W. and SW, Y.Y.: Investigating the dielectric effects of channel pore water on the electrostatic barriers of the permeation ion by the finite difference Poisson-Boltzmann method, *Eur. Biophys. J.* **27** (1998), 105–112.
16. Dieckmann, G.R., Lear, J.D., Zhong, Q., Klein, M.L., DeGradol, W.F. and Sharp, K.A.: Exploration of the structural features defining the conduction properties of a synthetic ion channel, *Biophys. J.* **76** (1999), 618–630.
17. Levitt, D.G.: Interpretation of biological ion channel flux data – Reaction-rate versus continuum theory, *Ann. Rev. Biophys. Chem.* **15** (1986), 29–57.
18. Eisenberg, R.S.: From structure to function in open ionic channels, *J. Membr. Biol.* **171** (1999), 1–24.
19. Nonner, W., Chen, D. and Eisenberg, B.: Anomalous mole fraction effect, electrostatics, and binding in ionic channels, *Biophys. J.* **74** (1998), 2327–2334.
20. Nonner, W. and Eisenberg, B.: Ion permeation and glutamate residues linked by Poisson-Nernst-Planck theory in L-type calcium channels, *Biophys. J.* **75** (1998), 1287–1305.
21. Nonner, W., Catacuzzeno, L. and Eisenberg, B.: Binding and selectivity in L-type calcium channels: a mean spherical approximation, *Biophys. J.* **79** (2000), 1976–1992.
22. Kurnikova, M.G., Coalson, R.D., Graf, P. and Nitzan, A.: A lattice relaxation algorithm for three-dimensional Poisson-Nernst-Planck theory with application to ion transport through the gramicidin A channel, *Biophys. J.* **76** (1999), 642–656.

23. Cardenas, A.E., Coalson, R.D. and Kurnikova, M.G.: Three-dimensional Poisson-Nernst-Planck theory studies: Influence of membrane electrostatics on gramicidin A channel conductance, *Biophys. J.* **79** (2000), 80–93.
24. Hollerbach, U., Chen, D.P., Busath, D.D. and Eisenberg, B.: Predicting function from structure using the Poisson-Nernst-Planck equations: Sodium current in the gramicidin A channel, *Langmuir* **16** (2000), 5509–5514.
25. Cooper, K.E., Jakobsson, E. and Wolynes, P.: The theory of ion transport through membrane channels, *Prog. Biophys. Mol. Biol.* **46** (1985), 51–96.
26. Li, S.C., Hoyles, M., Kuyucak, S. and Chung, S.H.: Brownian dynamics study of ion transport in the vestibule of membrane channels, *Biophys. J.* **74** (1998), 37–47.
27. Chung, S.H., Hoyles, M., Allen, T.W. and Kuyucak, S.: Study of ionic currents across a model membrane channel using Brownian dynamics, *Biophys. J.* **75** (1998), 793–809.
28. Roux, B. and Karplus, M.: Molecular dynamics simulations of the gramicidin channel, *Ann. Rev. Biophys. Biomol. Struct.* **23** (1994), 731–761.
29. Doyle, D.A., Cabral, J.M., Pfuetzner, R.A., Kuo, A., Gulbis, J.M., Cohen, S.L., Chait, B.T. and MacKinnon, R.: The structure of the potassium channel: molecular basis of K^+ conduction and selectivity, *Science* **280** (1998), 69–77.
30. Chang, G., Spencer, R.H., Lee, A.T., Barclay, M.T. and Rees, D.C.: Structure of the MscL homolog from *Mycobacterium tuberculosis*: A gated mechanosensitive ion channel, *Science* **282** (1998), 2220–2226.
31. Davis, M.E. and McCammon, J.A.: Electrostatics in biomolecular structure and dynamics, *Chem. Rev.* **90** (1990), 509–521.
32. Moy, G., Corry, B., Kuyucak, S. and Chung, S.H.: Tests of continuum theories as models of ion channels: I. Poisson-Boltzmann theory versus Brownian dynamics, *Biophys. J.* **78** (2000), 2349–2363.
33. Corry, B., Kuyucak, S. and Chung, S.H.: Tests of continuum theories as models of ion channels: 11. Poisson-Nernst-Planck theory versus Brownian dynamics, *Biophys. J.* **78** (2000), 2364–2381.
34. Hoyles, M., Kuyucak, S. and Chung, S.H.: Computer simulation of ion conductance in membrane channels, *Phys. Rev. E* **58** (1998), 3654–3661.
35. Corry, B., Allen, T.W., Kuyucak, S. and Chung, S.H.: Mechanisms of permeation and selectivity in calcium channels, *Biophys. J.* **80** (2001), 195–214.
36. Roux, B. and MacKinnon, R.: The cavity and pore helices in the KcsA K^+ electrostatic stabilization of monovalent cations, *Science* **285** (1999), 100–102.
37. Chung, S.H., Allen, T.W., Hoyles, M. and Kuyucak, S.: Permeation of ions across the potassium channel: Brownian dynamics studies, *Biophys. J.* **77** (1999), 2517–2533.
38. Chung, S.H., Allen, T.W. and Kuyucak, S.: Conducting-state properties of the KcsA potassium channel from molecular and Brownian dynamics simulations, *Biophys. J.*, **82** (2002), 628–645.
39. Cuello, L.G., Romero, J.G., Cortes, D.M. and Perozo, E.: pH dependent gating in the Streptomyces lividans K^+ channel, *Biochemistry* **37** (1998), 3229–3236.
40. Heginbotham, L., LeMasurier, M., Kolmakova-Partensky, L. and Miller, C.: Single Streptomyces lividans K^+ channels. Functional asymmetries and sidedness of proton activation, *J. Gen. Physiol.* **114** (1999), 551–559.
41. Roux, B., Bernèche, S. and Im, W.: Ion channels, permeation, and electrostatics: insight into the function of KcsA, *Biochemistry* **39** (2000), 13295–13306.
42. Allen, T.W., Kuyucak, S. and Chung S.H.: Molecular dynamics study of the KcsA potassium channel, *Biophys. J.* **77** (1999), 2502–2516.
43. Allen, T.W., Bliznyuk, A., Rendell, A.P., Kuyucak, S. and Chung, S.H.: The potassium channel: structure, selectivity and diffusion, *J. Chem. Phys.* **112** (2000), 8191–8204.
44. Tsien, R.W., Hess, P., McCleskey, E.W. and Rosenberg, R.L.: Calcium channels: Mechanisms of selectivity, permeation and block, *Ann. Rev. Biophys. Chem.* **16** (1987), 265–290.

45. McCleskey, E.W. and Almers, W.: The Ca channel in skeletal muscle is a large pore, *Proc. Natl. Acad. Sci. USA* **82** (1985), 7149–7153.
46. Yang, J., Ellinor, P.T., Sather, W.A., Zhang, J.F. and Tsien, R.W.: Molecular determinants of Ca^{2+} selectivity and ion permeation in L-type Ca^{2+} channels, *Nature* **366** (1993), 158–161.
47. Almers, W., McCleskey, E.W. and Palade, P.T.: A non-selective cation conductance in frog muscle membrane blocked by micromolar external calcium ions, *J. Physiol.* **353** (1984), 565–583.
48. Polo-Parada, L. and Korn, S.J.: Block of N-type calcium channels in chick sensory neurons by external sodium, *J. Gen. Physiol.* **109** (1997), 693–702.